

Nominal Controller Design Based on Decentralized Integral Controllability in the Framework of Reconfigurable Fault-Tolerant Structures

P. A. Luppi,^{†,‡} R. Outbib,^{†,§} and M. S. Basualdo^{*,†,||}

[†]CAPEG - CIFASIS (CONICET - UNR - AMU), 27 de Febrero 210 bis (S2000EZP), Rosario, Argentina

[‡]FCEIA, Universidad Nacional de Rosario, Pellegrini 250 (S2000EZP), Rosario, Argentina

[§]Laboratoire des Sciences de L'Information et des Systemes (LSIS), Aix Marseille Universite, Avenue Escadrille Normandie Niemen 13397, Marseille, France

^{||}Universidad Tecnologica Nacional - FRRO, Zeballos 1341 (S2000BQA), Rosario, Argentina

ABSTRACT: A reconfigurable fault-tolerant control system typically includes a nominal controller (NC), a fault detection/diagnosis (FDD) and decision subsystem, a reconfiguration mechanism, and a reconfigurable controller (RC). Here, a systematic methodology for designing a fully decentralized NC of reduced dimension is presented, providing (i) fault-tolerant capability due to the structural flexibility and (ii) availability of redundancies for RC design. The fulfillment of a sufficient condition for decentralized integral controllability is searched to guarantee the stability while the FDD scheme is identifying the faults. A novel framework based on a genetic algorithm is developed for obtaining alternative NCs. They are screened considering quantitative measures derived from stability and performance considerations. The procedure features complexity reduction because (i) it only utilizes steady-state process information and (ii) it is independent from the controller design. The methodology is tested in the Tennessee Eastman process to demonstrate its potential against set point/disturbance changes and stuck actuator faults.

1. INTRODUCTION

A fault-tolerant control (FTC) structure has been defined as one that is able to maintain the process stability and acceptable dynamic performance subject to malfunctions in system components.¹ Over the last years, significant research in FTC design have been developed in order to increase the safety and the reliability of industrial plants.^{2,3} In Figure 1, a typical (reconfigurable) FTC system architecture is shown, which is composed of a nominal controller (NC), a fault detection/diagnosis (FDD) and decision subsystem, a reconfiguration mechanism, and a reconfigurable controller (RC). In this framework, Luppi et al.⁴ presented a novel FTC design methodology which allows the NC structure to be reconfigured. It is based on the individual steady-state squared deviations in the context of the internal model control theory. An efficient management of the available healthy components is performed when actuator blockade or loss of sensor measurement occurs. In addition, a basic reconfiguration mechanism which minimizes the switching transients was implemented.

Here, the contribution is focused on an improved design of the NC structure, in order to guarantee certain stability properties, and overall performance. For this purpose, a novel procedure to obtain a set of candidate control structures which can fit well in industrial processes is presented. The proposal takes into account (i) a fully decentralized design, consisting of independent single input–single output (SISO) control loops, (ii) a unified framework for selecting the controlled variables (CVs), the manipulated variables (MVs), and the corresponding pairings, (iii) an analysis based on necessary/sufficient conditions for decentralized integral controllability (DIC) to assess the candidate solutions. As stated by Downs and

Skogestad,⁵ tools and techniques to carry out the design of control structures are very important in applications.

Although multivariable controllers can generally improve the closed-loop performance of large-scale processes, they involve complex design and implementation, including model development, which can be expensive and time-consuming.⁶ In contrast, decentralized control presents several advantages, making it the most used strategy. Due to its inherent flexibility in operation, it can provide fault-tolerant capability.⁷ Through the activation/deactivation of individual controllers, it is possible to easily modify the control structure. This was shown in Luppi et al.⁴ where a basic reconfiguration mechanism was utilized for accommodating typical faults. In this paper, the objective is to design a square decentralized structure for meeting all process requirements by using a minimum number of sensors and actuators. This leads to having the availability of redundancies which enables the FTC system to deal with different fault scenarios.⁸

A key stage in designing decentralized structures is the pairing between the MVs and the CVs. In most works, a fixed selection with the same number of MVs and CVs is established (generally based on engineering judgment) and the definition of the structure is only concerned with the pairing assignment. In this work, the variables selection and the pairing task are integrated and solved simultaneously. If there are considerable process interactions, providing alternative pairings for different

Received: April 23, 2014

Revised: December 8, 2014

Accepted: December 15, 2014

Published: December 16, 2014

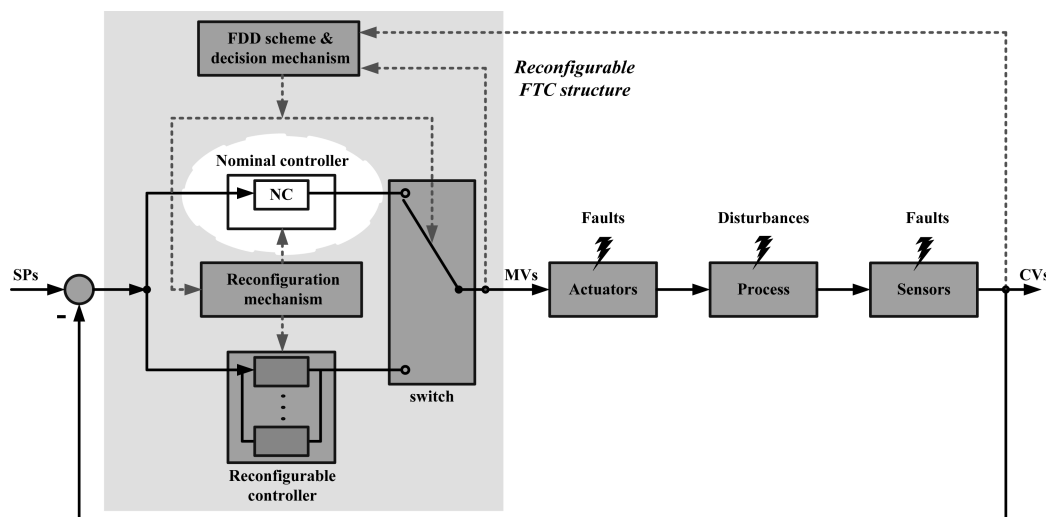


Figure 1. Typical reconfigurable FTC system.

candidate sets of CVs and MVs represents a complex problem, even for medium-scale systems. Since the adoption of an exhaustive search clearly becomes not practical, some systematic procedure to discard unsuitable solutions is requested. Here, the criteria to screen and evaluate candidate structures is based on stability and performance considerations, as explained in section 2.

A significant property of a process associated with a given diagonal control structure is the decentralized integral controllability (DIC), which was first presented by Skogestad and Morari.⁹ It determines that a decentralized controller with integral action in each loop (to ensure offset-free operation) will remain stable when any subset of loops is detuned or taken out of service.⁶ A typical example of the latter corresponds to stuck actuators, a hard fault scenario which is considered in this work.¹⁰ In practical applications, many operating constraints can be violated some time before the RC can be implemented, due to stability problems. In this context, a NC structure which satisfies the DIC property can guarantee the overall stability while the FDD scheme is identifying the fault. This behavior cannot be ensured in most of the existing reconfigurable FTC, as stated by Yu and Jiang.¹¹ In relation to the DIC property, several necessary/sufficient conditions were developed.^{6,7,12,13} Particularly, some of them are based on interaction measures. In effect, the DIC property was associated with the diagonal dominance concept.^{6,14} Despite the significant computational load demanded by medium/large scale systems, these methods present interesting characteristics resulting in complexity reduction:⁷ (i) they can be verified only with the steady-state gain matrix of the process and (ii) they determine certain closed-loop behavior which only depends on the selected diagonal structure, independently of the design of the controller itself. The present proposal integrates quantitative measures derived from the above criteria in a genetic algorithm (GA) based framework. The aim is to provide a systematic approach for screening alternative decentralized structures. Most preliminary works only utilized the necessary conditions for DIC to eliminate unworkable designs. Here, the GA searching process is driven to find, if they exist, solutions which meet a sufficient condition for DIC. This produces decentralized structures with the desired closed-loop characteristics in the context of FTC systems.

In summary, concerning the design of the NC, the new algorithm improves the previous proposal presented in Luppi et al.⁴ by incorporating the check of (i) a necessary condition for diagonal dominance at steady state,¹⁵ (ii) the determinant condition for integrity,⁶ and (iii) a sufficient condition for decentralized integral controllability.^{9,16} These conditions are included in steps 4–7 (section 2.2). They are considered by the new algorithm in order to find solutions which ensure stability in spite of specific instrumentation faults. This element constitutes the main contribution with respect to Luppi et al.⁴ In addition, a novel trade-off analysis comprising dimension, performance, and stability indexes is proposed to evaluate alternative designs.

The methodology is completely evaluated in the well-known Tennessee Eastman (TE) test problem introduced by Downs and Vogel¹⁷ because it is a well-known benchmark, accessible by the entire process control community. Nevertheless, the proposed systematic procedure, which minimizes the use of heuristic criteria, was designed to be generalized and can be applied in other processes. The performance of the proposed NC design and other solutions are compared through closed-loop simulations of the rigorous model. This is done by disturbing the system at the base case (mode 1) with the set point and load changes recommended by Downs and Vogel.¹⁷ In addition, the stability behavior is analyzed under several fault scenarios. The time response of key process variables as suggested by Downs and Vogel¹⁷ is presented. Finally, the integral absolute error (IAE) and the error improvement percent (EIP) are used for comparison purposes and to support the conclusions.

Mainly, the contributions of this work are (i) a novel procedure for NC design in the context of reconfigurable fault-tolerant structures, (ii) a unified framework for selecting the CVs, the MVs, and the corresponding pairings, (iii) consideration of the necessary/sufficient conditions for DIC together with performance issues, (iv) a methodology that only takes into account steady-state information, and that is independent from the controller design, and (v) performance of a dynamic evaluation on a well-known case study, subject to typical set point/disturbance changes and critical faults.

The paper is organized as follows: The next section details the design approach, presenting its background/tools and implementation. Section 3 starts with a brief description of the

TE process and some related preliminary remarks. It continues with the application of the methodology in order to design the NC structure. A complete closed-loop analysis taking into account dynamic performance and stability behavior is included in section 3.3. Finally, in section 4, the conclusions are exposed.

2. DESIGN METHODOLOGY

In the following, some steady-state tools are considered which constitutes the background of the proposed design procedure.

2.1. Background and Tools. Consider a stabilized process G , with n inputs and m outputs. For a suitable (square) selection of q inputs and q outputs (named here as G_s), the proposal is to control it by using a stable diagonal controller, with integral action in all outputs (for instance, decentralized SISO PI loops). For an appropriate CV–MV pairing, assume that the columns/rows of G_s are arranged to group the selected elements along the diagonal. In addition, \tilde{G}_s is a $q \times q$ diagonal matrix which contains the diagonal elements of G_s . Within this framework, Skogestad and Postlethwaite⁶ defined

$$E = (G_s - \tilde{G}_s) \tilde{G}_s^{-1} \quad (1)$$

where E represents a normalization (with respect to the diagonal elements) of the interactions caused by the off-diagonal elements of G_s . For a diagonal control structure, the input–output pairings are critical in order to minimize the effect of such interactions, which could produce instability. In the context of FTC, a stable closed-loop behavior is desired once particular actuator/sensor faults affect the system, and the corresponding controllers are taken out of service. This system property was called *integrity*. Furthermore, Skogestad and Morari⁹ introduced the stronger concept of *decentralized integral controllability* (DIC) related to a process G_s and the corresponding pairing selection, as commented in section 1. In order to measure the degree of interaction, the *structured singular value* of E , called $\mu(E)$ was introduced.¹⁴ Moreover, the concept of *diagonal dominance* was utilized to mean that the interactions do not introduce instability. In this context, Braatz¹⁶ demonstrated that a sufficient condition for DIC is that G_s is diagonally dominant at steady state, i.e., $\mu[E(0)] < 1$. An excellent review of conditions for DIC is given in Skogestad and Postlethwaite⁶ and Campo and Morari.⁷

On the other hand, the performance of the designed structures can be analyzed via the sum of square deviations.^{18,19} This well-known index evaluates the steady-state error related to the uncontrolled variables, assuming perfect control for the selected CVs. Then, many candidate solutions can be discarded at the early stage because unacceptable dynamic evolutions can be predicted through this index.⁴

2.2. Proposed Approach. The main steps are schematically given in Figure 2, comprising the following:

1. For a given stabilized G process ($m \times n$), propose alternative selections (G_{sk}) of q CVs and q MVs (q is the dimension of the structure). Here, q can take values between q_0 and $q = \min(m, n)$, where q_0 represents the minimum number of outputs that must be controlled due to process requirements. For a chosen q , there are $(m!/(m-q)!q!)(n!/(n-q)!q!)$ possible selections of G_s . Obviously, performing an exhaustive selection is impractical for the case of medium/large scale plants. Thus, a GA-based approach is proposed in the next section.

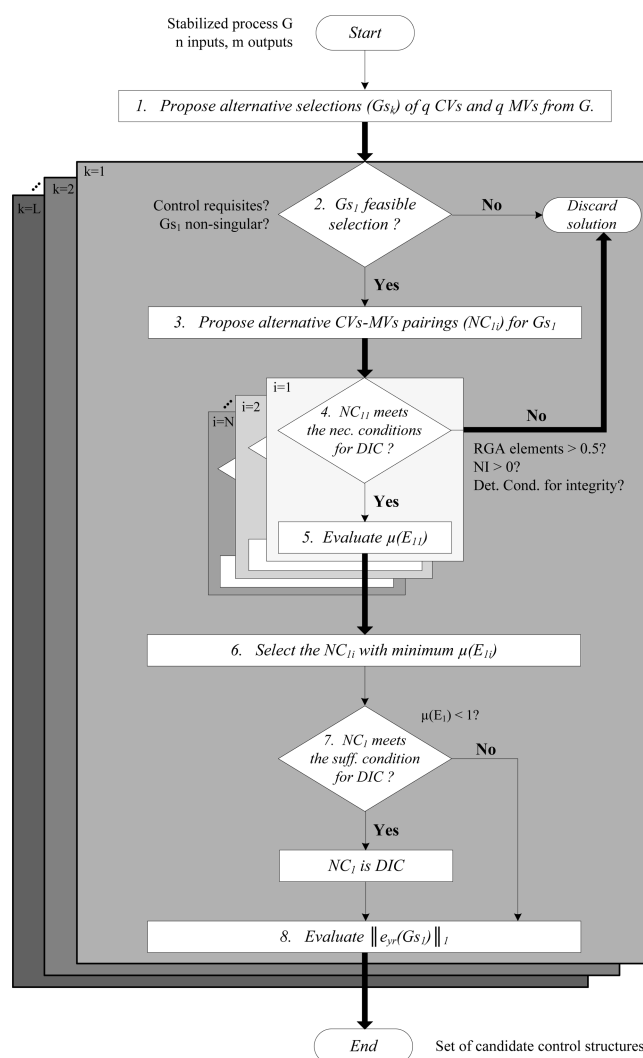


Figure 2. Proposed design approach.

2. Analyze the feasibility of the actual selection of G_{sk} considering the following:

- a. Are the outputs related to the process requirements selected as CVs?
- b. Is G_{sk} nonsingular? That is, is $\det(G_{sk}) \neq 0$?

As described in section 2.3, the requirement of item 2.a can be easily satisfied through a convenient GA parametrization. On the other hand, item 2.b corresponds to a necessary and sufficient condition for using integral control in all outputs.⁷ In addition, it enables the index calculation proposed in item 8.

3. If the current selection of G_{sk} is feasible, then propose alternative CV–MV pairings (NC_{ki}). For a selected G_{sk} , there are $q!$ possible pairings. Again, this represents a major complexity for large-scale plants. Thus, some criterion for supporting the pairing task is indispensable such that designs with unacceptable closed-loop behavior can be discarded. Several methods are available to solve this problem, and most of them are based on the well-known steady-state RGA:

- a. The iterative RGA (IRGA) can be used to obtain a pairing which satisfies the diagonal dominance property.⁶ However, it is possible to obtain a pairing associated with negative RGA

elements through this procedure, which is not desired (see item 4.a). For instance, this occurs when applying the IRGA to the CV selection proposed by Molina et al.¹⁹ for the TE base case.

- b. Another pairing procedure is based on the minimization of the RGA number.⁶ Here, the problem is that a small RGA number does not always guarantee diagonal dominance.⁶ In this context, Kariwala and Cao²⁰ proposed a branch and bound (BAB) based biobjective optimization algorithm in which the pairings can be selected from a Pareto optimal set by trading-off the RGA number and the $\mu(E)$ interaction measure. A significant advantage of this approach is that BAB methods provide global optimization for combinatorial problems.
- c. Mapping each RGA element through a particular nonlinear function drives to the normalized RGA (NRGA).^{21,22} Then, the pairing selection can be obtained from the solution of a conditional assignment problem. This procedure can prevent the choice of pairings with negative RGA elements. The NRGA approach can be solved with the Hungarian algorithm.²³ This is computationally efficient for large-scale systems.²² However, this methodology does not involve the fulfillment of other criteria (for instance, a positive Niederlinski index, see item 4.b). This could require several search-check-search loops to find suboptimal pairings which satisfy the above requirement.

In Appendix A, a brief review about the calculation of the RGA number, the IRGA, and the NRGA is detailed.

4. For each alternative (reordered) pairing, check the necessary conditions for DIC:
 - a. All diagonal elements of the RGA must be larger than 0.5 (this corresponds to a necessary condition for diagonal dominance at steady state).¹⁵
 - b. The NI of G_{sk} and the NI of each principal submatrix of G_{sk} must be positive (determinant condition for integrity).⁶

Those candidates which do not match these conditions can be eliminated.

5. If the current structure NC_{ki} satisfies the necessary conditions stated in item 4, then evaluate the corresponding $\mu(E_{ki})$.
6. From step 5, select the NC_{ki} with minimum $\mu(E_{ki})$. The objective is to find pairings such that G_{sk} meets (or gets closer to) the diagonal dominance property.
7. For the selected NC_k , check the sufficient condition for DIC, i.e., $\mu(E_k) < 1$. Note that NC_k could be DIC even if the above requirement is not satisfied.
8. Finally, calculate the sum of square deviations $\|e_{yr}(G_{sk})\|_1$.^{18,19} As stated earlier, the value of this index allows the performance of alternative structures to be compared.

Through this methodology, a set of candidate control structures which satisfy (at least) the necessary conditions for DIC is obtained. These solutions can be screened in an x - y axis graph ($\mu(E_k)$ vs $\|e_{yr}(G_{sk})\|_1$). Then, the final solution can be selected from the Pareto optimal set by trading off these two indexes (stability vs performance), as will be shown in section 3.2. Additionally, a closed-loop dynamic test must be performed

so as to verify that all control objectives are satisfied. This is detailed in section 3.3.

2.3. Implementation. As commented above, to perform every possible pairing for each potential set of CVs and MVs (i.e., exhaustive search) is not practical, even for medium-scale plants. In this work, a GA-based approach is employed because

- it is able to solve combinatorial problems of large dimension,
- it offers a set with the suboptimal solutions, and
- the risk of obtaining local optima is minimum.²⁴

GA is a stochastic global optimization procedure. It simulates the behavior of natural biological evolution, generating a certain number of optimization solutions.

In the context of GA, the methodology presented in section 2.2 is implemented through the following optimization problem. For a selected q (i.e., the structure dimension), the objective is to minimize the criterion given by eq 2 subject to the constraints of eqs 3–6:

$$\min_{(c_i^{cv}, c_i^{mv})} \mu[E(c_i^{cv}, c_i^{mv})] \quad (2)$$

subject to

$$\det[G_s(c_i^{cv}, c_i^{mv})] \neq 0 \quad (3)$$

$$\Lambda(j, j) > 0.5, \quad \text{with } j: 1, \dots, q \quad (4)$$

$$NI[G_s(c_i^{cv}, c_i^{mv})] > 0 \quad (5)$$

$$NI[G_s^{jj}(c_i^{cv}, c_i^{mv})] > 0, \quad \text{with } j: 1, \dots, q \quad (6)$$

where (c_i^{cv}, c_i^{mv}) represents the (binary) search chromosome. It has a length of $(m + n)$ genes corresponding to decision variables for the CVs and MVs. It is worth noting that the value of a particular gene can be directly set to 1 in order to force the selection of the corresponding variable (the selection will not change along the GA execution). This is usually employed to meet the requirement of item 2.a. According to item 2.b, the constraint of eq 3 guarantees that the variables selection is feasible. On the other hand, the inequalities of eqs 4, 5, and 6 correspond to the necessary conditions for DIC (item 4). Here, Λ represents the (reordered) steady-state RGA. In addition, $NI(G_s)$ and $NI(G_s^{jj})$ represent the Niederlinski index of G_s , and the j Niederlinski indices of all the principal submatrices of G_s , respectively, with

$$NI(G_s) = \frac{\det(G_s)}{\prod_j G_s(j, j)} \quad (7)$$

At each GA generation, the alternative CV–MV pairings (step 3) are obtained through the BAB solution proposed by Kariwala and Cao.²⁰ This algorithm is utilized here because

- it is useful for finding pairings such that the $\mu(E)$ measure be minimum for a selected G_s ,
- it provides global optimization, and
- it is computationally efficient.

In order to discard a solution (see steps 2 and 4 in section 2.2), the GA is programmed to assign an infinite value to the functional cost of eq 2. The advantage of the proposed GA implementation is that it minimizes the value of $\mu[E(c_i^{cv}, c_i^{mv})]$ after each generation and also reduces the percentage of discarded solutions during the search process.

3. APPLICATION CASE: TENNESSEE EASTMAN BENCHMARK PROBLEM

The industrial process control problem presented by Downs and Vogel¹⁷ is considered here for the purpose of evaluating the methodology described in section 2.

3.1. Preliminary Remarks. The well-known TE problem consists of five major units: a reactor, a product condenser, a vapor–liquid separator, a recycle compressor, and a product stripper. It involves two simultaneous exothermic reactions and also two additional byproduct reactions. The main process requirements are¹⁷ (i) to keep operating conditions within equipment constraints, (ii) to recover quickly from set point changes, (iii) to minimize the dynamic variability during disturbances, and (iv) to minimize the movement of valves. In the work of Downs and Vogel,¹⁷ a complete description of the TE process can be found. The complete list of variables is shown in Table 1. Additionally, the nomenclature used for all

Table 1. TE Process Variables

output	description	input	description
$xme(5)$	recycle flow (stream 8)	$xmv(1)$	D feed flow (stream 2)
$xme(6)$	reactor feed rate (stream 6)	$xmv(3)$	A feed flow (stream 1)
$xme(7)$	reactor pressure	$xmv(4)$	A and C feed flow (stream 4)
$xme(9)$	reactor temp.	$xmv(5)$	compressor recycle valve
$xme(11)$	product separator temp.	$xmv(6)$	purge valve (stream 9)
$xme(13)$	product separator pressure	$xmv(9)$	stripper steam valve
$xme(16)$	stripper pressure	$xmv(11)$	condenser cooling water flow
$xme(17)$	stripper underflow (stream 11)	$xme(21)_{sp}$	reactor cooling water outlet temp. set point
$xme(18)$	stripper temp.		
$xme(20)$	compressor work	$idv(1)$	A/C feed ratio (stream 4)
$xme(30)$	B comp. purge (stream 9)	$idv(2)$	B composition (stream 4)
$xme_{G/H}$	G/H comp. ratio (stream 11)		

the CVs, MVs, and DVs is the same as that given in Downs and Vogel.¹⁷ In this paper, it is assumed that the process operates at mode 1, i.e., the base case.¹⁷

3.1.1. Process Stabilization and Model Identification. First, the TE plant is open-loop unstable. In Molina et al.,¹⁹ it was determined that the reactor level ($xme(8)$), the product separator level ($xme(12)$), the stripper level ($xme(15)$), and the reactor cooling water outlet temperature ($xme(21)$) must be controlled in order to stabilize the process. The corresponding CV–MV pairing as well as the tuning parameters are indicated in Table 2. In addition, Figure 3 shows a detailed flow sheet of the plant where the stabilizing loops are depicted with a white background. These loops are selected from the beginning of the methodology presented in

Table 2. Stabilizing Control Loops

CV	MV	K_c	T_I
$xme(8)$	$xmv(2)$	9	1.7
$xme(12)$	$xmv(7)$	−0.1	2
$xme(15)$	$xmv(8)$	−0.12	7.5
$xme(21)$	$xmv(10)$	−1.7	0.03

section 2.2. This stabilization task has a significant influence on the remaining steps of the method. In fact, various degrees of freedom are blocked at this stage, thus eliminating many design alternatives.

As explained in Luppi et al.,²² certain system identification techniques can be applied to the stabilized nonlinear model of the process in order to obtain the steady-state gains corresponding to the input–output variables. Following a similar procedure, Zumoffen¹⁸ and Molina et al.¹⁹ estimated the normalized steady-state gain matrices G (inputs – outputs) and D (disturbances – outputs). These matrices are utilized in this work for supporting the controller design stage. The values of G and D are presented in Table 11.

3.2. Control Structure Design. A major consideration for the control structure design is that the reactor pressure ($xme(7)$), the stripper underflow ($xme(17)$), the B comp. purge ($xme(30)$), and the G/H comp. ratio ($xme_{G/H}$) must be controlled due to TE process requirements.¹⁷ In this regard, it is necessary to select $q - 4$ CVs from a total of $12 - 4 = 8$ available measurements and q MVs from eight available inputs, together with the $q \times q$ CV–MV pairing. In this context, the proposed methodology addresses square control design for typically nonsquare processes. The objective is to choose small values of q (i.e., to consider $q = 4, 5$, etc.) because a minimum number of CVs and MVs is preferred (structures of dimension $4 \times 4, 5 \times 5$, respectively). Then, it is proposed to solve the following problem:

- Problem 1

$$\min_{(C_i^*)} \mu[E(C_i^*)] \quad (8)$$

subject to

$$C_i^* = [c_i^{cv}(1:8), 1, 1, 1, 1, c_i^{mv}(1:8)] \quad (9)$$

$$\sum_{k=1}^8 c_i^{cv}(k) = q - 4 \quad \text{and} \quad \sum_{j=1}^8 c_i^{mv}(j) = q \quad (10)$$

$$\det[G_s(C_i^*)] \neq 0 \quad (11)$$

$$\Lambda(j, j) > 0.5, \quad \text{with } j: 1, \dots, q \quad (12)$$

$$NI[G_s(C_i^*)] > 0 \quad \text{and} \quad NI[G_s^{jj}(C_i^*)] > 0, \quad \text{with } j: 1, \dots, q \quad (13)$$

Here, C_i^* represents the searched chromosome which has a length of 20 (binary) genes. It has 12 decision variables for the CVs (corresponding to $xme(5)$, $xme(6)$, $xme(9)$, $xme(11)$, $xme(13)$, $xme(16)$, $xme(18)$, $xme(20)$, $xme(7)$, $xme(17)$, $xme(30)$, and $xme_{G/H}$) and 8 decision variables for the MVs ($xmv(1)$, $xmv(3)$, $xmv(4)$, $xmv(5)$, $xmv(6)$, $xmv(9)$, $xme(21)_{sp}$, and $xmv(11)$); see Table 1. The components $c_i^{cv}(1:8)$ and $c_i^{mv}(1:8)$ from eq 9 represent the genes corresponding to $xme(5)$ – $xme(20)$ and $xmv(1)$ – $xmv(11)$, respectively. They can individually take values of 0 or 1 along the GA execution. However, the genes corresponding to $xme(7)$, $xme(17)$, $xme(30)$, and $xme_{G/H}$ (positions 9, 10, 11, and 12 in C_i^*) are forced to be 1; i.e., these outputs are forced to be selected as CVs.

With the settings described in Table 3, the GA was executed several times to find solutions to

- Problem 1 with $q = 5$

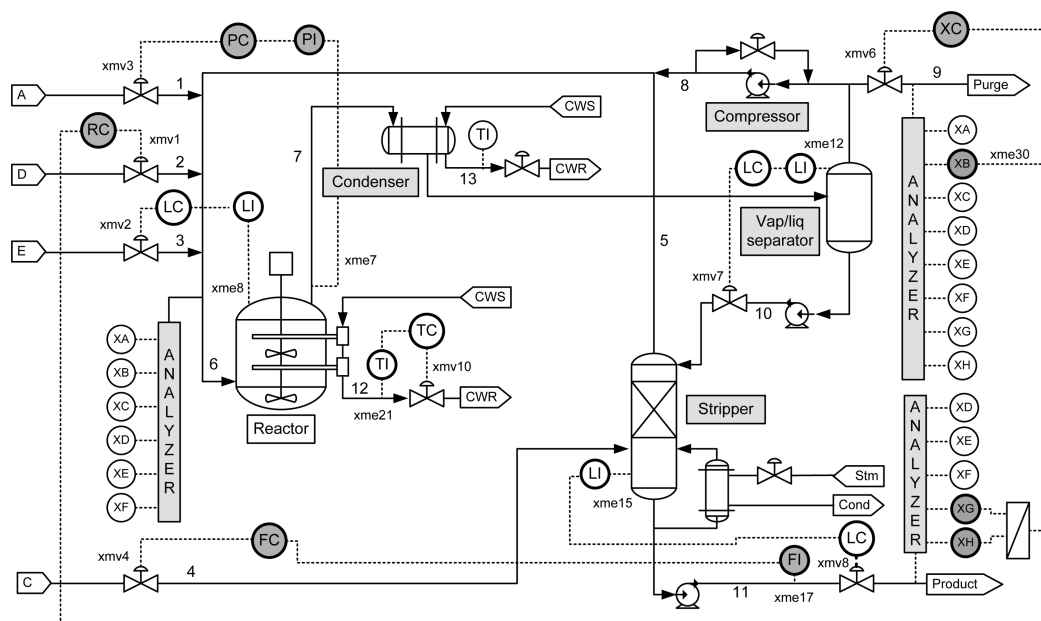


Figure 3. TE flow sheet. Stabilizing loops and nominal controller NC_5 .

Table 3. Genetic Algorithm Parameters

parameter	value
initial population, N_i	10 000
chromosome length, N_c	20
no. of generations, N_g	50
mutation probability	$0.7/N_c$
crossover probability	0.7
selection method	roulette wheel

• Problem 1 with $q = 4$

The problem was solved using only $q = 4$ or $q = 5$ because the objective is to fulfill all the process requirements by using the minimum number of control loops. As stated in Luppi et al.,⁴ in the context of FTC systems, this ensures that (i) the amount of sensors and actuators that can fail during process operation is minimized and (ii) the number of available redundancies necessary for the next stage of the methodology, i.e., the RC design, is maximized. The diversity of failure scenarios that the FTC system is able to face depends strongly on these additional healthy components.^{3,8} From a more general point of view, both investment and operating costs can

be severely impacted if the proposed design does not use the minimum number of control loops to meet all the process objectives.¹⁸

The obtained solutions are presented in parts a (5×5 structures) and b (4×4 structures) of Figure 4. These plots can be used for evaluating alternative control structures. The following criteria are proposed to eliminate designs: (i) solutions with $\mu[E(C_i^*)] > 1$, (ii) solutions with large $\|e_{yr}(C_i^*)\|_1$, and (iii) solutions not belonging to the Pareto optimal set.

After this analysis, only five alternatives can be considered as candidate control structures: the 5×5 structures NC_1 , NC_2 , and NC_3 , and the 4×4 structures NC_4 and NC_5 . Table 4 presents the CV–MV pairings corresponding to these configurations. In addition, Table 5 shows the $\|e_{yr}(C_i^*)\|_1$ and the $\mu[E(C_i^*)]$ obtained for each solution. As concluded in section 3.3.1, the NC_5 will be selected as the final solution due to the good trade-off comprising performance, dimension, and stability properties. It is shown in Figure 3 where the proposed controllers are highlighted with a gray background.

3.3. Closed-Loop Analysis. 3.3.1. Dynamic Performance. In this section, the closed-loop performance of the obtained

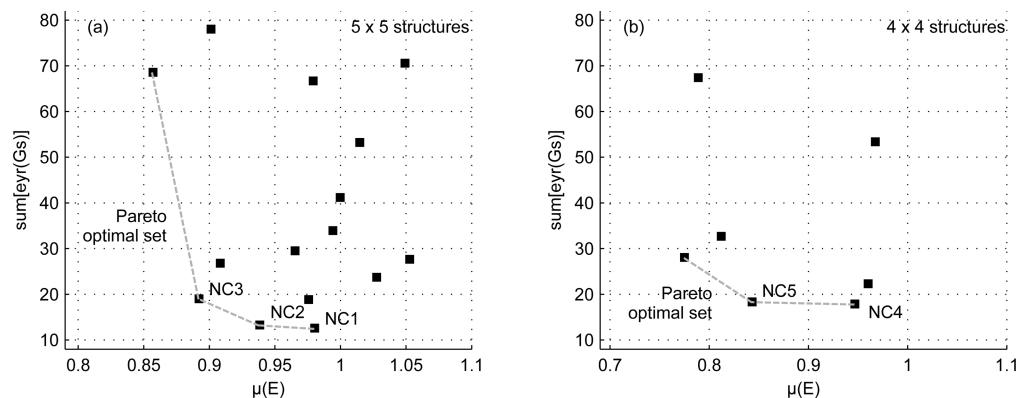


Figure 4. Alternative solutions: (a) 5×5 structures; (b) 4×4 structures.

Table 4. Alternative Solutions

	NC ₁	NC ₂	NC ₃	NC ₄	NC ₅
q:	5	5	5	4	4
	$xmv(1)-xme_{G/H}$	$xmv(1)-xme_{G/H}$	$xmv(1)-xme_{G/H}$	$xmv(1)-xme_{G/H}$	$xmv(1)-xme_{G/H}$
	$xmv(4)-xme(17)$	$xmv(3)-xme(7)$	$xmv(3)-xme(7)$	$xmv(4)-xme(17)$	$xmv(3)-xme(7)$
	$xmv(6)-xme(7)$	$xmv(4)-xme(17)$	$xmv(4)-xme(17)$	$xmv(6)-xme(7)$	$xmv(4)-xme(17)$
	$xmv(9)-xme(18)$	$xmv(6)-xme(30)$	$xmv(9)-xme(18)$	$xme(21)sp-xme(30)$	$xmv(6)-xme(30)$
	$xme(21)sp-xme(30)$	$xmv(9)-xme(18)$	$xme(21)sp-xme(30)$		

Table 5. Alternative Solutions. Stability and Performance Measures

	NC ₁	NC ₂	NC ₃	NC ₄	NC ₅
q:	5	5	5	4	4
$\mu[E(C_i^*)]$	0.98	0.93	0.89	0.94	0.84
$\ e_{yr}(C_i^*)\ _1$	12.60	13.28	19.02	17.89	18.33

control structures is evaluated through a complete set of simulations. For the purpose of comparing results, the process is disturbed at the base case (mode 1) with the set point changes and the disturbances described in Table 6, as proposed by Downs and Vogel.¹⁷ On the other hand, as required in Downs and Vogel,¹⁷ a qualitative comparison of the time responses of key process variables is presented. To this end, two well-known indexes are considered: (i) the IAE, i.e., the integral absolute error, and (ii) the EIP, i.e., the error improvement percent, where

$$IAE = \int_{t_1}^{t_2} |e(t)| dt \quad (14)$$

with

$$e(t) = r(t) - y(t) \quad (15)$$

Here, $r(t)$ represents the nominal value (or set point) and $y(t)$ denotes the process output. On the other hand, $[t_1, t_2]$ corresponds to the evaluation period. In addition,

$$EIP = \frac{IAE^{base} - IAE^{new}}{IAE^{base}} \times 100 \quad (16)$$

where “base” represents the control structure considered as a reference and “new” denotes an alternative solution to be evaluated. The IAE and EIP indexes can be calculated for all outputs. Note that, if the EIP index results in being positive, then the new control strategy is better than the base one. As suggested in Downs and Vogel,¹⁷ these indexes are calculated for the following variables: $xme(1)$, $xme(2)$, $xme(3)$, $xme(4)$, $xme(7)$, $xme(17)$, $xme_{G/H}$, and also the operating costs. The corresponding results are shown in Tables 7, 9, and 10, where

NC₅ is considered the base structure in order to calculate the EIP and NC₂ and NC_M constitute alternative solutions to be analyzed (NC_M corresponds to the control strategy proposed by Molina et al.¹⁹). Furthermore, the designed structures are implemented with SISO PI controllers. The corresponding parameters were selected according to the procedure presented in Rivera²⁵ and are shown in Table 8.

First, it is worth mentioning that structures NC₁, NC₃, and NC₄ are not suitable. This is because a shutdown is produced when the process is subjected to disturbances $idv(1)$, $idv(2)$, and $idv(1)$, respectively.

On the contrary, NC₂ and NC₅ comply with all the set point/disturbance scenarios. Figures 5–7 depict some regulatory responses corresponding to key variables of the process, where the NC₅ structure is confronted with other candidate solutions. Note that the tracking behavior is not shown because there are no appreciable differences in the dynamics of $xme(7)$, $xme(17)$, $xme(30)$, and $xme_{G/H}$ when the associated set point modifications occur. Parts a and b of Figure 5 show the dynamics of the stripper underflow ($xme(17)$) and the G/H comp. ratio ($xme_{G/H}$). The NC₅ presents good regulatory behavior subject to $idv(1)$ – $idv(4)$, with an acceptable increase in the IAE value with respect to the strategy of Molina et al.:¹⁹ $EIP(xme(17)) = -14.94\%$ and $EIP(xme_{G/H}) = -16.90\%$ (see Table 10). In parts a and b of Figure 6, the E feed (stream 3) ($xme(3)$) and the reactor pressure ($xme(7)$) responses are shown, respectively. The NC₅ and the structure proposed by Molina et al.¹⁹ are compared under the $idv(8)$ – $idv(12)$ scenario. The NC₅ demonstrates a great performance for $xme(3)$, with a reduction of 47.20% in the IAE with respect to the strategy of Molina et al.¹⁹ On the other hand, it shows a very small IAE increase ($EIP = -2.98\%$) for $xme(7)$ (see Table 10). Apart from this, the stripper steam flow ($xme(19)$) is shown in Figure 7. Taking into account this variable, the new strategy NC₅ (4×4) presents excellent performance when compared against NC₂ (5×5): $EIP(xme(19)) = 333.02\%$ for $idv(1)$ – $idv(4)$ (scenario 5) and $EIP(xme(19)) = 350.41\%$ for $idv(8)$ – $idv(12)$ (scenario 6).

Table 6. Set Point Changes and Disturbances

scenario	time (h)	event	process var.	type	magnitude
1	10	reactor op. pressure change	$xme(7)$	step	−3%
2	10	production rate change	$xme(17)$	step	−15%
3	10	purge gas B comp. change	$xme(30)$	step	+14%
4	10	product mix change	$xme_{G/H}$	step	50G/50H to 45G/55H
	50	product mix change	$xme_{G/H}$	step	45G/55H to 50G/50H
5	0–22	A/C feed ratio, B comp. const. (str. 4)	$idv(1)$	step	enabled
	50–100	reactor cooling water inlet temp.	$idv(4)$	step	enabled
6	10–40	A, B, C feed comp. (stream 4)	$idv(8)$	random	enabled
	60–90	condenser cooling water inlet temp.	$idv(12)$	random	enabled

Table 7. Dynamic Performance Comparison. Scenarios 1 and 2 (Set Point Changes)

scenario:	1: $xme(7)_{sp}$ step			2: $xme(17)_{sp}$ step		
	NC_5	NC_2	NC_M	NC_5	NC_2	NC_M
	IAE	EIP	EIP	IAE	EIP	EIP
$xme(1)$	2.78×10^2	0.06	N/C	5.12×10^2	−0.43	37.10
$xme(2)$	1.94×10^5	0.86	N/C	4.48×10^6	−1.06	0.55
$xme(3)$	1.21×10^6	−0.56	N/C	5.29×10^6	−2.09	−7.74
$xme(4)$	5.49×10^2	6.37	N/C	1.17×10^4	−1.03	0.18
$xme(7)$	5.88×10^4	0.59	N/C	5.34×10^4	0.47	−92.65
$xme(17)$	1.08×10^3	0.35	N/C	3.49×10^3	−0.10	−1.50
$xme_{G/H}$	1.80×10^2	0.32	N/C	2.29×10^2	−0.08	−8.01
op. costs	1.74×10^6	−0.04	N/C	1.68×10^6	0.37	6.97

Table 8. Implemented SISO PI Controllers

MV	CV	K_c	T_i
$xmv(1)$	$xme_{G/H}$	9.5	1
$xmv(3)$	$xme(7)$	−0.2	10
$xmv(4)$	$xme(17)$	1.5	1
$xmv(6)$	$xme(7)$	−0.35	20
$xmv(6)$	$xme(30)$	−2.7	2
$xmv(9)$	$xme(18)$	7.9	0.2
$xme(21)_{sp}$	$xme(30)$	0.25	0.33

Even though NC_2 increases the dimension of the structure, it does not propose a noticeable improvement of the dynamics with respect to NC_5 . This is reflected by the small EIP values of Tables 7, 9, and 10. For this reason, both structures manifest almost equal operating costs. Taking into account the control requirements stated in section 3.1, the NC_5 is the smallest possible decentralized structure (4×4). Given its excellent balance between overall performance/stability and dimension, the NC_5 was proposed as the final solution (see also section 3.3.2).

3.3.2. Stability Behavior. Consider the CV selection proposed by Molina et al.¹⁹ for the base case: $xme(5)$, $xme(11)$, $xme(13)$, $xme(18)$, $xme(20)$, $xme(17)$, $xme(30)$, and $xme_{G/H}$. Taking into account all degrees of freedom ($xmv(1)$ to $xmv(11)$), the following CV–MV pairing is suggested here: $xme(5)$ – $xmv(11)$, $xme(11)$ – $xme(21)_{sp}$, $xme(13)$ – $xmv(3)$, $xme(18)$ – $xmv(9)$, $xme(20)$ – $xmv(5)$, $xme(17)$ – $xmv(4)$, $xme(30)$ – $xmv(6)$, and $xme_{G/H}$ – $xmv(1)$ (this structure is named here as NC_6). Although the diagonal elements of the rearranged RGA are all positive for this case (1.26, 0.34, 1.11, 1.87, 1.18, 1.10, 0.19, 1.05), the NC_6 does not satisfy the necessary conditions for DIC, since $NI = -2.62$. In the following, the stability behavior of NC_5 (it satisfies the sufficient

condition for DIC), the structure presented by Zumoffen¹⁸ (it satisfies the necessary conditions for DIC) and NC_6 (it does not satisfy the necessary conditions for DIC) are compared under several fault scenarios.

The first simulation corresponds to a fault in the A feed flow (stream 1) manipulated variable ($xmv(3)$), called F_1 . In this case, a sticking which occurs at $t = 5$ h was considered. Figure 8a shows the dynamic behavior of the F comp. (stream 9) ($xme(34)$) at the nominal operating point. It can be seen that NC_6 can no longer guarantee the stability once F_1 appears. Figure 8b depicts the stripper steam flow ($xme(19)$). Unlike NC_6 , the structure presented by Zumoffen¹⁸ and also NC_5 can still maintain the stability of the postfault system (NC_5 dynamics are not depicted in Figure 8b because there are no appreciable differences with the work of Zumoffen¹⁸).

The second simulation case is presented in Figure 9 and considers a fault in the A and C feed flow (stream 4) manipulated variable ($xmv(4)$), called F_2 . A sticking at $t = 12.5$ h which occurs after a set point change in $xme_{G/H}$ (50G/50H to 45G/55H at $t = 10$ h) was considered. Figure 9a shows the E comp. (stream 11) ($xme(38)$) dynamics. When F_2 is present, the structure NC_6 cannot preserve the stability of the system. Finally, in Figure 9b, the B comp. (stream 6) ($xme(24)$) is shown. In contrast to NC_6 , the NC_5 configuration maintains the stability of the process after the occurrence of F_2 .

4. CONCLUSIONS

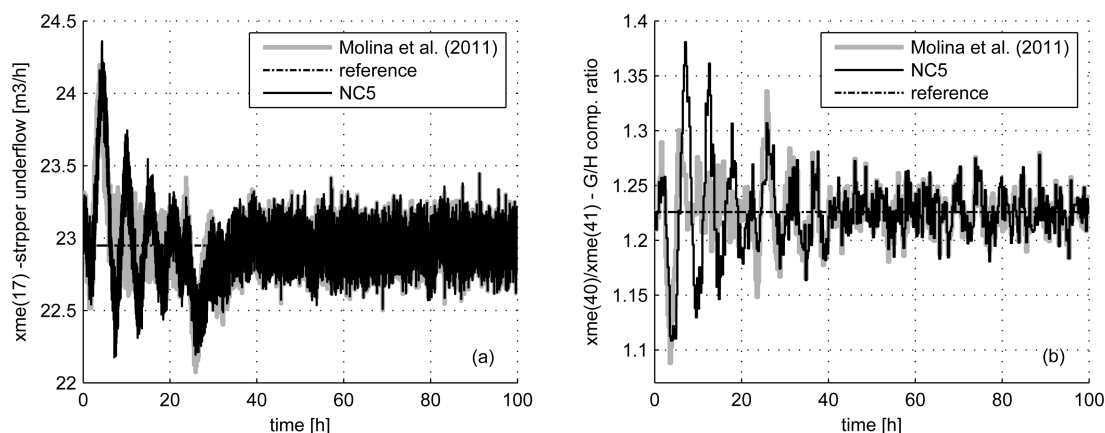
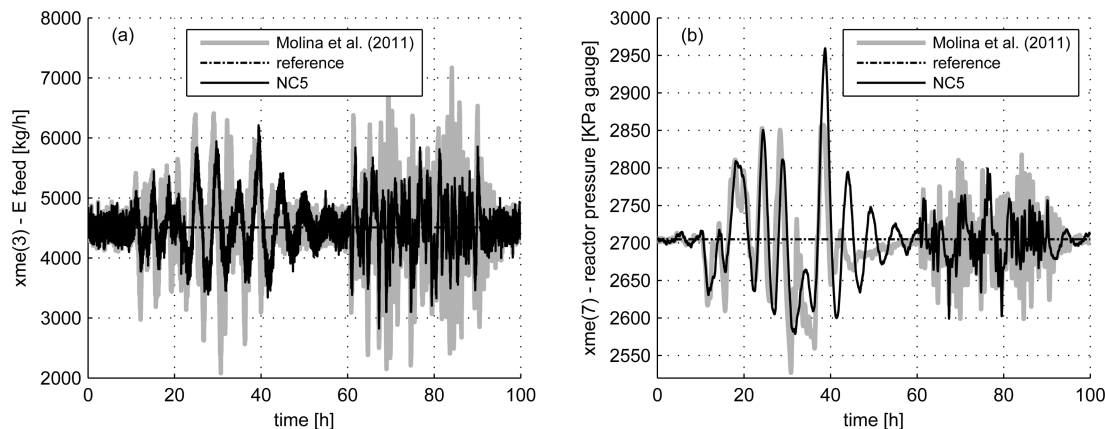
Through the TE case study, it was demonstrated that the proposed methodology produces suitable decentralized control structures for reconfigurable FTC systems. The obtained results indicate that the implemented solution (NC_5) ensures acceptable performance subject to typical set point/disturbance scenarios. Moreover, NC_5 properly handles critical stuck actuator faults, which bring the corresponding control loop

Table 9. Dynamic Performance Comparison. Scenarios 3 and 4 (Set Point Changes)

scenario:	3: $xme(30)_{sp}$ step			4: $xme_{G/H} sp$ step		
	NC_5	NC_2	NC_M	NC_5	NC_2	NC_M
	IAE	EIP	EIP	IAE	EIP	EIP
$xme(1)$	1.44×10^2	0.28	25.68	2.54×10^2	−0.17	29.68
$xme(2)$	1.83×10^5	−0.21	0.01	1.56×10^6	−0.99	−2.51
$xme(3)$	1.12×10^6	0.04	−2.02	2.58×10^6	1.37	−1.72
$xme(4)$	6.04×10^2	−0.71	−2.61	7.92×10^2	−5.23	−13.57
$xme(7)$	4.36×10^4	1.04	22.94	8.00×10^4	−0.14	33.04
$xme(17)$	9.97×10^2	0.21	1.71	1.16×10^3	0.05	5.20
$xme_{G/H}$	1.61×10^2	0.36	3.95	2.63×10^2	−0.29	3.86
op. costs	1.57×10^6	0.00	−0.94	1.72×10^6	0.05	−2.74

Table 10. Dynamic Performance Comparison. Scenarios 5 and 6 (Disturbances)

scenario:	5: $idv(1)$, $idv(4)$ (step)			6: $idv(8)$, $idv(12)$ (random)		
	NC_5	NC_2	NC_M	NC_5	NC_2	NC_M
	IAE	EIP	EIP	IAE	EIP	EIP
$xme(1)$	1.26×10^3	0.06	0.13	7.52×10^2	-0.17	13.63
$xme(2)$	2.57×10^5	0.12	11.74	3.67×10^5	0.71	11.76
$xme(3)$	1.51×10^6	-1.38	6.37	3.24×10^6	0.68	-47.20
$xme(4)$	1.54×10^3	-0.34	-2.96	8.65×10^2	0.82	14.79
$xme(7)$	4.55×10^5	0.04	-0.44	3.62×10^5	-0.13	2.98
$xme(17)$	1.59×10^3	-1.39	14.94	2.34×10^3	2.27	18.09
$xme_{G/H}$	2.50×10^2	-0.74	16.90	4.57×10^2	0.90	10.80
op. costs	1.70×10^6	-0.02	-0.57	1.72×10^6	0.01	-0.33

Figure 5. $xme(17)$ and $xme_{G/H}$ dynamic responses. Scenario 5: $idv(1)$ – $idv(4)$ disturbances.Figure 6. $xme(3)$ and $xme(7)$ dynamic responses. Scenario 6: $idv(8)$ – $idv(12)$ disturbances.

out of service. In this regard, the stability is guaranteed on the basis of the fulfillment of a sufficient condition for DIC. It is worth mentioning that NC_5 (4 PI loops + 4 stability loops) is the smallest decentralized structure that can be found in the literature.^{18,19,26–28} In addition, acceptable computation time was required by the proposed GA implementation for solving the CV and MV selection together with the CV–MV pairings. On the other hand, a brief discussion about alternative pairing techniques was presented. Clearly, a systematic pairing procedure results indispensable if certain closed-loop characteristics are desired for the system.

The methodology drives to a decentralized control structure which can be initially implemented through conventional PID controllers. In a subsequent stage, any other control strategy

such as feedforward controllers and Smith predictors can be easily included to improve the dynamic performance of the system. On the other hand, if it is desired to implement cascade control, consider that (i) once the process is stabilized the inner loops must be defined and for this purpose heuristic/engineering criteria could be used, (ii) then obtain the steady-state model G (inputs – outputs), where the set points of the inner loops must be considered as model inputs, and (iii) execute the procedure described in section 2.2 by forcing the selection of the inner loop set points as manipulated variables so as to obtain the cascade loops. The analysis of the DIC property must be performed on square $q \times q$ selections which involve the conventional PID loops and also the outer loops of

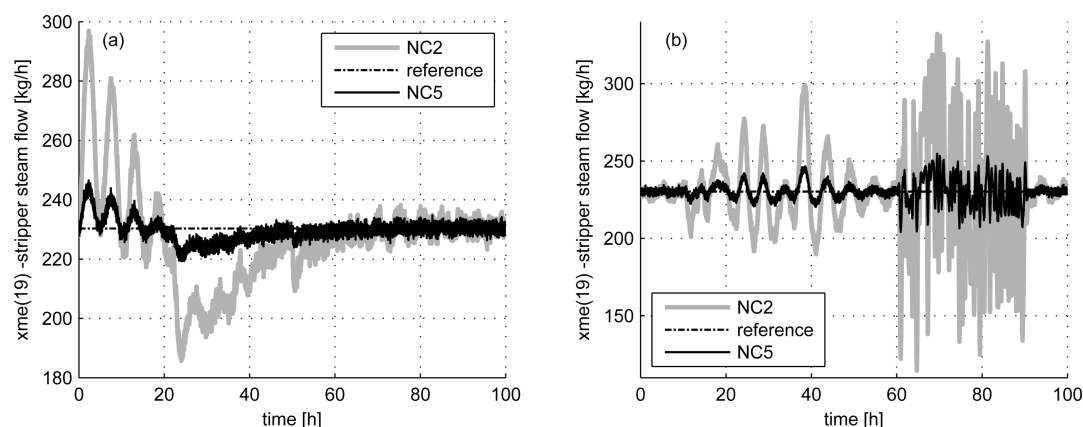


Figure 7. $xme(19)$ dynamic responses: (a) scenario 5; (b) scenario 6.

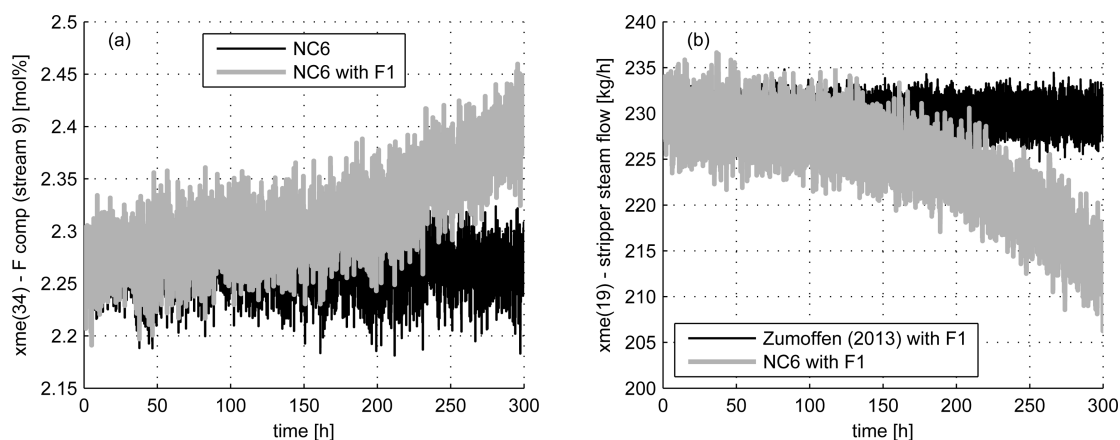


Figure 8. $xme(34)$ and $xme(19)$ dynamic responses. Fault F_1 : A feed flow ($xmv(3)$) sticking at $t = 5$ h.

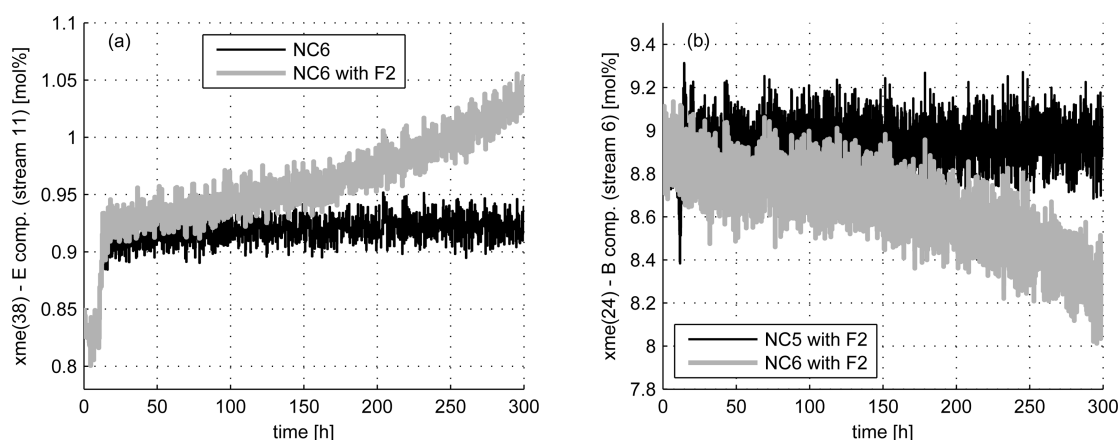


Figure 9. $xme(38)$ and $xme(24)$ dynamic responses (scenario 4: product mix change at $t = 10$ h). Fault F_2 : A and C feed flow ($xmv(4)$) sticking at $t = 12.5$ h.

the cascades. Concerning the latter loops, the aim is to ensure the system stability when they are switched to manual mode.

In general, every design procedure involves defining its range of validity. The proposed method allows one to design NC structures which guarantee the overall stability for a wide range of typical fault scenarios, such as (i) any actuator blockade, (ii) loss of measurement of any sensor, (iii) detuning of any control loop, and (iv) the above events acting in sequence and/or simultaneously. However, other type of events such as plant faults could occur. In general, for this case, the current design

cannot ensure stability. Future work will be focused on extending the methodology so as to guarantee stability (when possible) for a defined set of critical process faults. Regardless of its great potential, the method generates NC structures which depend on the considered faults at the design stage. If a different fault occurs, the behavior of the process will be unknown. For selecting the critical fault scenarios, it is recommendable to perform a risk analysis. A useful method is the HAZOP analysis which is typically utilized in chemical industries. It is usually developed by a group of professionals

Table 11. TE Normalized Steady-State Gain Matrices G (Inputs – Outputs) and D (Disturbances – Outputs)

	G								D	
	$xmv(1)$	$xmv(3)$	$xmv(4)$	$xmv(5)$	$xmv(6)$	$xmv(9)$	$xme(21)_{sp}$	$xmv(11)$	$idv(1)$	$idv(2)$
$xme(5)$	−0.38	−0.02	−0.11	0.06	−0.13	−0.02	0.78	−0.08	0.59	0.54
$xme(6)$	−0.36	0.00	0.10	0.09	−0.13	−0.03	0.69	−0.08	0.65	0.49
$xme(9)$	0.26	0.02	0.60	−0.08	0.04	0.05	−0.77	0.01	−1.02	−1.04
$xme(11)$	0.38	0.06	0.21	−0.10	0.08	0.04	−0.80	−0.04	−0.94	−1.08
$xme(13)$	−0.43	−0.12	0.43	0.10	−0.20	0.01	0.56	−0.04	0.97	1.08
$xme(16)$	−0.43	−0.12	0.44	0.07	−0.20	0.00	0.55	−0.04	0.97	1.08
$xme(18)$	0.38	0.06	0.22	−0.09	0.08	0.10	−0.78	−0.07	−0.97	−1.08
$xme(20)$	−0.37	0.03	−0.01	0.20	−0.10	−0.04	0.78	−0.13	−1.29	0.96
$xme(7)$	−0.43	−0.12	0.43	0.09	−0.20	0.01	0.56	−0.04	0.98	1.08
$xme(17)$	−0.02	0.02	0.70	−0.01	0.02	0.01	−0.11	0.00	−0.20	−0.05
$xme(30)$	0.43	0.00	0.25	−0.13	−0.18	0.01	−0.84	0.06	−1.03	1.06
$xme_{G/H}$	0.60	−0.03	−0.53	0.02	0.00	0.00	0.00	−0.01	0.55	0.08

who have experience in design, operation, and maintenance of plants.

Finally, in order to meet the operating conditions specified in the design, industrial processes usually require large amounts of energy. The synthesis stage plays a key role in minimizing the initial investment costs as well as the operation costs. On the other hand, the installed process equipment can introduce important interactions which affect the dynamic behavior of the plant. In this regard, an incorrect selection of process design parameters could greatly complicate the control problem. Future work will be focused on the analysis of new alternatives for integrating the design of reconfigurable control structures with the process synthesis stage. The aim is to make the entire process operate at a high efficiency operating point, by tolerating critical fault scenarios.

APPENDIX A

Consider a square matrix G_s such that the selected pairings are positioned on the diagonal. Then, the RGA number is defined as⁶

$$\text{RGA number} = \|\Lambda(G_s) - I\|_{\text{sum}} \quad (17)$$

where $\|A\|_{\text{sum}} = \sum_{ij} |a_{ij}|$, Λ represents the RGA, and I is the identity matrix.

On the other hand, the iterative RGA (IRGA) corresponds to a sequential evaluation of the RGA, i.e., $\Lambda^2(G_s) = \Lambda[\Lambda(G_s)]$, etc. It was demonstrated that Λ^k converges to the identity matrix I if G_s is diagonally dominant.²⁹ Typically, Λ^k converges to I for k between 4 and 8.⁶

Finally, the normalized RGA (NRGA) is obtained by mapping each element λ_{ij} of the RGA through a certain nonlinear function f . In Fatehi and Shariati²¹ and Luppi et al.,²² the following function was used for NRGA:

$$f(\lambda_{ij}) = \begin{cases} 0 & \text{if } \lambda_{ij} \leq 0 \\ \lambda_{ij} & \text{if } 0 < \lambda_{ij} \leq 1 \\ e^{(1-\lambda_{ij})/4} & \text{if } 1 < \lambda_{ij} \end{cases} \quad (18)$$

APPENDIX B

The values of G and D are presented in Table 11.

AUTHOR INFORMATION

Corresponding Author

*E-mail: basualdo@cifasis-conicet.gov.ar.

Notes

The authors declare no competing financial interest.

ACKNOWLEDGMENTS

The authors thank ANPCyT (Agencia Nacional de Promoción Científica y Técnica), UNR-FCEIA (Universidad Nacional de Rosario), and CONICET (Consejo Nacional de Investigaciones Científicas y Técnicas) for the financial support. The authors also acknowledge the support from UTN-FRRO (Universidad Tecnológica Nacional) and CAPEG-CIFASIS (Computer Aided Process Engineering Group - Centro Internacional Franco Argentino de Ciencias de la Información y de Sistemas).

REFERENCES

- (1) Patton, R. Fault-tolerant Control: The 1997 Situation. *3rd IFAC Symposium on fault detection, supervision and safety for technical processes*. 1997, 1033–1055.
- (2) Mhaskar, P.; Liu, J.; Christofides, P. *Fault-Tolerant Process Control. Methods and Applications*; Springer: London, England, 2013.
- (3) Zhang, Y.; Jiang, J. Bibliographical review on reconfigurable fault-tolerant control systems. *Annu. Rev. Control* 2008, 32, 229–252.
- (4) Luppi, P.; Nieto Degliuomini, L.; Garcia, M.; Basualdo, M. Fault-tolerant control design for safe production of hydrogen from bio-ethanol. *Int. J. Hydrogen Energy* 2014, 39, 231–248.
- (5) Downs, J.; Skogestad, S. An industrial and academic perspective on plantwide control. *Annu. Rev. Control* 2011, 35, 99–110.
- (6) Skogestad, S.; Postlethwaite, I. *Multivariable feedback control. Analysis and design*; John Wiley & Sons: Chichester, England, 2005.
- (7) Campo, P.; Morari, M. Achievable closed-loop properties of systems under decentralized control: conditions involving the steady-state gain. *IEEE Trans. Autom. Control* 1994, 39, 932–943.
- (8) Jiang, J.; Yu, X. Fault-tolerant control systems: A comparative study between active and passive approaches. *Annu. Rev. Control* 2012, 36, 60–72.
- (9) Skogestad, S.; Morari, M. Variable selection for decentralized control. *AIChE Annual Meeting*, Washington, DC, 1988, 128c.
- (10) Chen, W.; Jiang, J. Fault-tolerant control against stuck actuator faults. *IEE Proc.: Control Theory Appl.* 2005, 152, 138–146.
- (11) Yu, X.; Jiang, J. Hybrid Fault-Tolerant Flight Control System Design Against Partial Actuator Failures. *IEEE Trans. Control Syst. Technol.* 2012, 20, 871–886.
- (12) Bao, J.; McLellan, P.; Forbes, J. A passivity-based analysis for decentralized integral controllability. *Automatica* 2002, 38, 243–247.

- (13) Lee, J.; Edgar, T. Conditions for decentralized integral controllability. *J. Process Control* **2002**, *12*, 797–805.
- (14) Grosdidier, P.; Morari, M. Interaction measures for systems under decentralized control. *Automatica* **1986**, *22*, 309–319.
- (15) Kariwala, V.; Forbes, J.; Meadows, E. Block relative gain: properties and pairing rules. *Ind. Eng. Chem. Res.* **2003**, *42*, 4564–4574.
- (16) Braatz, R. Robust Loopshaping for Process Control. Ph.D. Thesis, California Institute of Technology, 1993.
- (17) Downs, J. J.; Vogel, E. F. A plant-wide industrial process control problem. *Comput. Chem. Eng.* **1993**, *17*, 245–255.
- (18) Zumoffen, D. Oversizing analysis in plant-wide control design for industrial processes. *Comput. Chem. Eng.* **2013**, 145–155.
- (19) Molina, G.; Zumoffen, D.; Basualdo, M. Plant-wide Control Strategy Applied to the Tennessee Eastman Process at Two Operating Points. *Comput. Chem. Eng.* **2011**, 2081–2097.
- (20) Kariwala, V.; Cao, Y. Branch and Bound method for multiobjective pairing selection. *Automatica* **2010**, *46*, 932–936.
- (21) Fatehi, A.; Shariati, A. Automatic Pairing of MIMO Plants Using Normalized RGA. Mediterranean Conference on Control and Automation, **2007**, T07–005.
- (22) Luppi, P.; Zumoffen, D.; Basualdo, M. Decentralized plantwide control strategy for large-scale processes. Case study: Pulp mill benchmark problem. *Comput. Chem. Eng.* **2013**, 272–285.
- (23) Cooper, L.; Steinberg, D. *Methods and Applications of Linear Programming*; Saunders: Philadelphia, Pennsylvania, USA, 1974.
- (24) Sharifzadeh, M.; Thornhill, N. Optimal selection of control structure using a steady-state inversely controlled process model. *Comput. Chem. Eng.* **2012**, 126–138.
- (25) Rivera, D. Internal Model Control. PID Controller Design. *Ind. Eng. Chem. Process Des. Dev.* **1986**, *25*, 252–265.
- (26) Banerjee, A.; Arkun, Y. Control configuration design applied to the Tennessee Eastman plant-wide control problem. *Comput. Chem. Eng.* **1995**, *19*, 453–480.
- (27) Ricker, N. Decentralized control of the Tennessee Eastman challenge process. *J. Process Control* **1996**, *6*, 205–221.
- (28) Larsson, T.; Hestemtum, K.; Hovland, E.; Skogestad, S. Self-optimizing control of a large-scale plant: the Tennessee Eastman process. *Ind. Eng. Chem. Res.* **2001**, *40*, 4889–4901.
- (29) Johnson, C.; Shapiro, H. Mathematical aspects of the relative gain array. *SIAM J. Algebraic Discrete Methods* **1986**, *7*, 627–644.